Plasma Confinement in the WIIa-Stellarator: A Comparison between Experimental Results and Theoretical Estimates of "Neoclassical" Diffusion

D. Eckhartt

IPP 2/86

July 1970

INSTITUT FÜR PLASMAPHYSIK

GARCHING BEI MUNCHEN

INSTITUT FÜR PLASMAPHYSIK

GARCHING BEI MÜNCHEN

Plasma Confinement in the WIIa-Stellarator: A Comparison between Experimental Results and Theoretical Estimates of "Neoclassical" Diffusion

D. Eckhartt

IPP 2/86 July 1970

Die nachstehende Arbeit wurde im Rahmen des Vertrages zwischen dem Institut für Plasmaphysik GmbH und der Europäischen Atomgemeinschaft über die Zusammenarbeit auf dem Gebiete der Plasmaphysik durchgeführt.

IPP 2/86 D. Eckhartt

Plasma Confinement in the WIIa-Stellarator: A Comparison between Experimental Results and Theoretical Estimates of "Neoclassical" Diffusion

July 1970
(in English)

Abstract

Experiments with plasmas generated by contact ionization, photo ionization, and electron cyclotron resonance heating in the stellarator WIIa are reviewed. The magnitude of cross field particle diffusion observed in these experiments is compared with theoretical estimates of "neoclassical" diffusion. The scaling of these estimates from presently available plasma densities and temperatures towards higher temperatures predicts an increase in the diffusion rate, in contrast to what is expected from hydromagnetic theory (Pfirsch-Schlüter coefficient).

1. Introduction

Plasma confinement in most stellarator experiments has been found to be much worse than predicted from hydromagnetic theory.[1,2] Attempts to clarify this disagreement have been mainly directed towards the search for microinstabilities, since the plasmas under investigation exhibited a high degree of small scale fluctuations.[3] It was only during the past two or three years that it has been fully recognized, that the estimates on confinement from hydromagnetic theory give an upper limit and apply to the case of very short collision free paths.[4] These conditions could be achieved in the low density low temperature plasmas produced by contact ionization in the "Wendelstein" W I and W II stellarators.[5,6]

In the present report the experiments with contact ionized and photo ionized barium plasmas in the W IIa stellarator are reviewed. Next, we discuss results from preliminary measurements with plasmas generated by low power c.w. electron cyclotron resonance heating.[7] In the following chapters, the observed confinement times are compared with estimates of neoclassical diffusion derived from the theory of Kovrizhnik.[8] Finally, the magnitude of the neoclassical diffusion coefficient in regimes of higher plasma density and temperature is evaluated.

2. Contact Ionized Barium Plasmas

The confinement of low density low temperature barium plasmas has been studied using plasma production by contact ionization.[6] Peak densities were in the range 3×10^8 to 5×10^9 cm^{-3}. The lower limit in density was determined by the accuracy of the density detecting system which utilizes resonance fluorescence scattering of an incident light beam by the Ba^+-ions. The upper density limit is given by the temperature of the contact ionization source (emitter) together with the condition that it must be operated in the "electron-rich" regime. This implies that the rate of thermal electron emission from the emitter must be larger than the rate of ion production by a factor which is several times the square root of the mass ratio between ions and electrons. The base pressure during operation was usually

several times 10^{-7} torr measured by a Bayard Alpert gauge with standard calibration for air. Hence the degree of ionization in the central plasma region varied between 1 and 15 percent. The electrons were assumed to have a Maxwellian velocity distribution with a corresponding temperature equal to that of the emitter. This assumption was inferred from Q-machine theory but has never been checked by measurements during the experiments discussed here. The ions were assumed to have a similar velocity distribution plus a superimposed velocity component directed along the magnetic field which they gain when running "downhill" the potential sheath around the emitter in the electron rich-regime. The ion production rate or ion input flux could be measured with relative ease. All measurements were carried out in steady state operation. Hence, the maximum values of the main magnetic field, B_o, and of the rotational transform, ι[x)], were limited by power and cooling requirements. Normal operating conditions were B_o = 5 Kgauss with $\iota \leq 0.5$ and a measurement of B_o = 7.5 Kgauss with $\iota \leq 0.2$.

From these experiments the following results have been obtained:

(a) Dependence of Density on Rotational Transform

When ion input flux and main magnetic field are kept constant, the n vs. ι-curves follow a characteristic pattern.[9] Beyond a certain lower limiting value in ι the density starts to build up and - upon slowly increasing the helical currents - shows a series of maxima and minima. The envelope curve connecting the maxima passes through a maximum and has an ι-dependence which can be qualitatively understood since with increasing ι the confinement improves and the volume of the limiting magnetic surface shrinks. The density minima occur at a series of ι-values which lies close to the set of rational fractions, $\frac{m}{n}$, $m < n$, where m and n are not too large integers. For these specific values of ι the magnetic surfaces should degenerate and - as the lines of force in this stellarator have only a small amount of shear - this degeneracy should extend over a considerable part of the entire plasma volume.

---

x) ι is defined as $\frac{\ell}{2\pi}$ where ℓ is the angle of rotational transform around the machine.

Attempts to explain the lower limit in ι of the observed density onset and of the steep rise in density after its onset have been along two lines of argumentation: "lack of equilibrium" and "thermalization" of the ions. Lack of equilibrium [10] in this context, means that the magnitude of the secondary currents (proportional to $1/\iota$) is so high that their resistive voltage drop across the magnetic field induces an ExB-plasma-motion which is too large to be compensated by mass flow along the magnetic lines of force. The question of thermalization of ions [11] is connected with the Q-machine mode of plasma production together with poor plasma confinement al low ι's. Under these conditions the particle life time is short and the plasma density low. Hence, the potential drop in the emitter sheath is rather high. This, in turn, gives the ions a high directed velocity which makes it difficult for them during their short life time, to get thermalized through collisions with plasma particles already trapped. Once the density has been raised above a certain value, the voltage drop and the directed ion velocity decrease, the collision probability becomes higher thus further increasing the density. An abrupt density rise would be expected and has been observed. Both afore mentioned ideas remained in a qualitative stage and have never been developped into a rigorous theory for the low density regime considered. Their range of validity, therefore, remains unknown.

The density minima, or "holes", occur under quite general plasma conditions, they are also observed in ECR generated plasmas as will be discussed in Chapter 6. Similar effects have been found in the L-1 stellarator with gun-produced plasmas. [12] In the latter machine, electron beam studies have revealed a break-up of magnetic surfaces at rational values of ι. Similar measurements in the W IIa stellarator are highly desirable in order to study the magnetic topography for "rational surfaces" and, in particular, to answer the question why the minima occur for values of ι which are slightly different from those expected on the basis of numerical field calculations and the magnitudes of the currents through the main and helical field windings.

The general shape of the n vs. ι-curves can be influenced by a radial electric field without change of the location of the minima. This electric field is set up by applying a voltage between the vacuum vessel and the emitter which - under normal condition - is insulated and on floating voltage. The role of

this externally applied electric field and that of eventually drawn plasma currents is unknown and should be subject of more systematic investigations.

Additional magnetic fields directed either in the equatorial plane or perpendicular to it, lead to a change of the general shape of the n vs. t-curves as well as of their detail structure. Again, the resulting magnetic field topology should be studied by means of the electron beam method.

The occurence of enhanced plasma losses for "rational surfaces" immediately raises the question about plasma confinement in stellarator fields where the magnetic lines of force have shear in order to suppress instabilities. These sheared fields form nested surfaces with neighbouring "rational" and "non-rational" surfaces. The straight-forward question is whether or not in such a stellarator configuration the "bad" confinement properties of rational surfaces would still persist. To investigate this question a new device of the W II-series is under construction. Neighbouring "rational" and "non-rational" magnetic surfaces are an intrinsic property of multipole configurations with superimposed toroidal fields. The outcome of confinement studies with such systems will be of interest, therefore, in particular those of the Princeton "Spherator".[13]

(b) Absence of Fluctuations

It has been possible to achieve experimental conditions where the level of density fluctuations is remarkably low, perhaps in the order of 1 percent in the central plasma region. Theory would predict several modes of micro-instabilities in the shear-free magnetic field.

(c) Confinement

For the experimental conditions mentioned in the preceding section, the steady state peak density varied as $\sqrt{\Phi}$ where Φ is the total ion input flux. Within the experimental errors there is no difference whether the density was measured by Langmuir probes or by resonance fluorescence spectroscopy. In the absence of probes (and supporting wires of the plasma emitter) the only plasma losses conceivable are recombination on the emitter and cross field particle losses. The recombination flux to the emitter is known from Q-machine theory to scale as n^2 for the operating conditions

in question, its magnitude is usually smaller than the total ion input flux. Hence, the cross field flux is found to vary as n^2. This dependence is expected for resistive diffusion across the magnetic confining field of a stellarator. For the case considered in Appendix I, the diffusion coefficient derived from the measurements, is about five to six times larger than the Pfirsch-Schlüter value, that is, for a fully ionized axisymmetric plasma with electron temperature equal to the emitter temperature.

The annular gridded particle detector inside the machine should allow an independent and absolute measurement of the cross field particle flux arriving at the outermost magnetic surfaces. Unfortunately, this device has never worked in a completely satisfactory manner.

If Bohm-diffusion would control the cross field particle losses, the cross field flux would be proportional to $D_B \cdot n$, where D_B is $\frac{c\,k\,T_e}{16\,e\,B}$. As mentioned previously, the electron temperature has never been measured. Let us assume, for a moment, that the electrons were at room temperature due to some rapid cooling process not yet specified. We then could ask how much cross field flux proportional to n could be added to the resistive loss flux ($\propto n^2$) such that the combined fluxes would still fit the observed n vs. Φ-curves within the experimental uncertainities. The result is that Bohm type diffusion proportional to $\frac{1}{10} \ldots \frac{1}{20}$ times D_B would be reconcilable with the experimental data. The rapid cooling assumed is hard to explain on the basis of presently available data on collision cross-sections of low energy electrons. On the other hand, the unknown "exotic" chemistry which probably takes place in these types of plasma, might well give reasons that the above arguments cannot be rejected without further considerations.

The average particle life time, τ, can be computed in these steady state experiments by dividing the total number of particles present in the machine by the particle input flux. On the basis of the radial density profile shown in Ref. 6 and the assumption of symmetry around the major circumference, one arrives at $\tau \approx 0{,}6$ sec. This life time scales as 1/n and therfore ranges from 6 to 0,4 sec for the present densities.

3. Plasma Production by Photo-ionization of Barium Atoms

It has been proposed[14] to dispense with the solid plasma emitter and its supports and to use photo-ionization of barium atoms by crossing a light beam with a flux of neutral atoms inside the stellarator W IIa. In the volume common to both beams the barium atoms will be ionized and the charged particles produced are trapped by the magnetic field. At the moment of production neither electrons nor ions have an equilibrium velocity distribution. The production rates can be measured by a method similar to that with contact ionized plasmas. Up to now production rates have been achieved which are smaller than expected: for a photo-ionized flux of about 10^{11} sec^{-1} the resulting peak particle density was $1{,}3 \cdot 10^{7}$ cm^{-3} being about 8 times less than predicted from the extrapolation of the n vs. Φ-curves measured in contact-ionized plasmas with the same background pressure. The n vs. t-dependence showed a pattern which resembles that observed with contact-ionized plasmas. The latter result again indicates that the occurence of minima at specific values of t is connected with the magnetic topography rather than with the method of plasma production.

4. Contact Ionized Plasmas with Sudden Removal of the Emitter

A device has been built which allows steady state plasma generation by contact ionization and subsequent extraction of the plasma emitter out of the confinement volume[14]. The mechanical extraction takes about 120 msec. Preliminary experiments show a distortion of the plasma during the withdrawal of the emitter: a transient signal appears at the particle detector indicating that a fraction of the plasma is removed. The central density behaves qualitatively as expected, it shows a rapid drop to about $^{2}/_{3}$ of its stationary value followed by a smooth decay. It should be possible to refine this method i.e., to measure the plasma decay in space and time and to compare the observations with numerical calculations of the decay process.

5. Application of "Mild Heating" to Plasmas Generated by Contact Ionization

Recent theories on the transport coefficients in plasmas where the collision mean free paths are long compared to the connection length R_o/t, have shown, that the diffusion coefficient is greater than expected from hydromagnetic theory, i.e. the Pfirsch-Schlüter value. In the contact ionized plasmas discussed in Chapter 2, the ratio of the mean free path for electron-ion collisions to connection length ranges from about $^1/_3$ to $^1/_{50}$. This ratio could be increased by raising the electron temperature since $\lambda_{ei} \propto T_e^2$. There is no obvious reason why this raise of electron temperature could not be done by the application of a "mild" and controllable method of plasma heating starting from a regime of "good" plasma confinement in contact ionized plasmas which are generated by the presently available machinery. Experiments with low power electron cyclotron resonance heating in a Q-machine gave quantitative agreement with theoretical expectations regarding heat conduction[15]. Heating by low power DC or AC Ohmic heating is also conceivable. This could be done with the emitter inside or with extracted emitter. In the latter case the starting conditions would be less defined. Experiments with ECR heated plasmas in W IIa which will be discussed in the following chapter, have shown that it is possible to generate and heat a steady noble gas plasma with microwave powers as low as 10 milliwatts entering the magnetic field volume. This power is negligible compared to the power which is radiated from the plasma emitter in steady state. Moreover, the emitter surface is less than 0.1 percent of the plasma aperture. Cross field heat conduction will certainly require additional microwave power if the emitter is left inside. The concept of a "point source" of plasma production has to be abandoned anyhow, since raising the electron temperature in order to increase the electron mean free path, inevitably increases the number of high energy electrons in the tail of the Maxwell distribution which are capable of generating ions by collisions with the background barium vapor atoms. To be more specific: in order to generate an equal amount of input ion flux by collisional ionization as that from presently available contact ionization, the electron temperature will be in the order of 2 to 3 eV. Hence, the electron mean free path will be increased by about two orders of magnitude. Such a increase would be desirable in order to keep track of

the predicted variation of the neoclassical diffusion coefficient. The problems of measuring the electron temperature, the additional production rate from collisional ionization, and the subsequent change in the radial density profile should not be too difficult.

6. ECR-Generated Noble Gas Plasmas

Preliminary measurements have been made in argon and xenon plasmas that were generated by c.w. low power microwave heating at frequencies corresponding to electron cyclotron resonance between 3,3 and 5,6 kilogauss.[7] Plasma densities and temperatures - both measured by Langmuir probes - were in the range 10^8 to 10^{11} cm^{-3} and, respectively, 4 to 12 eV. Hence, the degree of ionization varied between 2×10^{-2} percent and 60 percent, depending on neutral pressure and microwave power input. Decay measurements of the ion saturation current to the probe after switching off the microwave power showed, that the average plasma life time was in the order of 1 to 3 msec. This time was - in most cases - shorter than the electron-ion energy equipartition time. Therefore, the ion temperature presumably did not exceed the neutral gas temperature. The following plasma properties have been studied:

(a) n vs ι-Dependence

The n vs ι-curves in argon showed a similar pattern as those observed in barium plasmas. The width and depth of the density minima depend on neutral pressure and microwave power input. For high enough power input plasma could be produced at all values of ι including zero transform. This result is consistent with the assumption of reduced plasma confinement at the specific values of ι.

In particular, for medium microwave powers, a sudden density onset was observed followed by a steep density rise. This behaviour is quite similar to that observed in contact ionized plasmas, as discussed in Chapter 2, in spite of the completely different mechanism of plasma generation.

In xenon a range of discharge parameters was found where relative maxima of density appeared at rational ι-values superimposed to the general trend

of broad minima near $t = 1/3$ and $1/2$. Similar peaks have been observed in contact ionized plasmas when the background pressure was relatively high.[14] High pressure high power discharges in xenon showed a smooth n-t-curve.

(b) Fluctuations

The ECR-generated plasmas in general showed fluctuations in the frequency range expected for drift waves. The relative density variation $\frac{\delta n}{n}$ was in the order of 10 to 20 percent.

(c) Confinement

The average life time of the steadily operated plasmas has been determined from the total number of particles and the input flux or production rate, as it has been done in the case of barium plasmas produced by contact ionization. The input flux in ECR-generated plasmas, however, cannot be measured directly but must be inferred from measurements of power, density and electron temperature. An upper limit to the production rate can be estimated by assigning a certain energy, U[x], to each electron-ion pair produced and dividing the input power by U. This energy, U, in a global way takes into account the various inelastic processes and energy losses suffered by the electrons. A second and less formalistic way is to assume a Maxwellian distribution of electron energies and to compute the input flux from the known rate coefficients, $\overline{\sigma v_e}$, where the bar indicates an average over all electron energies for some specific temperature. The assumption of a Maxwell distribution of electron energies is subject to questions since one would expect the inelastic processes to deplete the tail of the energy distribution. Column 5 of Table I, where the estimates on confinement are summarized, shows that the production rates, $\dot{N}$, computed according to the two methods outlined above, agree satisfactorily well. The upper lines of this column refer to the evaluation from rate coefficients, the lower ones to that from input microwave power assuming U = 50 eV and taking all the microwave power that enters the discharge vessel. This value for U is somewhat higher than that known from literature [17] (i.e. twice the ionization potential) allowing for

---

x) U is sometimes called "mean energy of ionization".[16]

non-perfect absorption of the incident microwave power. The relevant discharge parameters are also listed in Table I and indicate that the present experiments include regimes where the electron-electron collision times are both longer and shorter than the average plasma life times.

7. Theoretical Estimates on Particle Diffusion in Axisymmetric Systems

In plasmas with long mean free paths for momentum transfer collisions the transport processes become more and more determined by those particles which are trapped in the mirrors of the toroidal magnetic field and make large excursions from their "starting" magnetic surface ("banana orbits"). With decreasing mean free path the diffusion rate also decreases and, in the limit, reaches the Pfirsch-Schlüter value derived from hydromagnetic plasma theory.

Since the first work by Galeev and Sagdeev[4] a number of papers have been published which confirm their results, apart from minor numerical disagreements. In the following, the theory of Kovrizhnik is[8] taken as a basis for numerical evaluation and comparison with the experimental results. It covers weakly as well as strongly ionized plasmas, the difference being that in fully ionized axisymmetric plasmas the diffusion rates for electrons and ions are equal whereas in weakly ionized plasmas an ambipolar electric field appears to equalize the different diffusion rates.

Upon inserting numerical values in the formulae given by Kovrizhnik, expressions for the diffusion coefficients in the W IIa machine are found for the various plasma conditions treated in the preceding chapters. Details are given in Appendix II. If a temperature gradient exists it is assumed $\frac{d(\ln n)}{dr} = \frac{d(\ln T)}{dr}$ in order to simplify the calculations. An exact derivation requires simultaneous solution of the energy transport equations given also by Kovrizhnik. The diffusion coefficient, D, is then expressed as a function of c_e, where $c_e = \frac{\lambda_e \cdot R_o}{v_e \cdot t} = \frac{R_o}{\lambda_e \cdot t}$, i.e., the inverse ratio of the mean free path for electron collisions and the connection length. Different expressions for D apply depending on the magnitude of c_e.

A. Contact Ionzied Plasmas, $T_e = T_i$

The following expressions are found for a fully ionized isothermal plasma:

$$D = \begin{cases} 1{,}38 \cdot \varrho_e^2 \cdot \dfrac{\nu_e}{R_o \cdot t} \cdot C_{ei} \\ \quad = 44{,}2 \cdot D_B \cdot \dfrac{\varrho_e}{R_o \cdot t} \cdot C_{ei} & 1 \ll C_{ei} \\ 100 \cdot D_B \cdot \dfrac{\varrho_e}{R_o \cdot t} & \frac{1}{2}\left(\frac{r_o}{R_o}\right)^{3/2} < C_{ei} < 1 \\ 216 \cdot D_B \cdot \left(\dfrac{R_o}{r_o}\right)^{3/2} \cdot C_{ei} \dfrac{\varrho_e}{R_o \cdot t} & C_{ei} \ll \left(\dfrac{r_o}{R_o}\right)^{3/2} \end{cases}$$

ϱ_e is the electron Larmor radius, R_o and r_o are major and minor plasma radius, respectively. By inserting the following numbers: B_o = 5 kilogauss, t = 0.1, R_o = 50 cm, R_o/r_o = 10 and choosing a value for the plasma temperature, one obtains D as function of peak particle density n_{eo}. Examples are shown in Fig. 1 as fully drawn curves. The curves for T = 0,2 eV and 2 eV include the plateau part of the curve typical for neoclassical diffusion with the plateau value independent of density. The broken lines show the influence of electron collisions with the rest gas atoms. This influence is taken into account in a first order approximation neglecting ambipolar effects, by multiplying the values of D with a factor $\frac{\nu_{ei} + \nu_{eo}}{\nu_{ei}}$. The values for ν_{eo} are taken from the literature [18] assuming air as rest gas at a pressure of 10^{-6} torr. At low values of n_e, and dependent on T_e, the diffusion coefficient becomes independent of the electron density. The dotted line represent the hydromagnetic (Pfirsch-Schlüter) value for T = 0,2 eV.

The experimentally observed values from Appendix I are shown as hatched area for the two values of emitter temperature usually considered. The agreement is good considering the various approximations and assumptions involved.

The calculated data are replotted in Fig. 2 to show the temperature dependence of D for various fixed peak densities. Again, the broken lines refer to the effect of electron neutral collisions and the dotted lines represent the

Pfirsch-Schlüter value. Starting from the plasma parameters of the contact ionization regime the diffusion coefficient increases with increasing temperature in contrast to what one would expect on the basis of the hydromagnetic plasma model.

B. ECR-Generated Plasmas, $T_e \gg T_i$

The average plasma life time τ has been determined for various discharges in argon which are listed in Table I. They include cases of high as well as of low degree of ionization. The criterion given by Kovrizhnik for weakly ionized plasmas:

$$\nu_{jn} \gg \nu_{ei} \left(\frac{R_o}{r_o}\right) \frac{m_e}{m_j} \frac{T_e + T_i}{T_j} \quad , \qquad j = e, i$$

is satisfied by the cases 1, 2, and 6. None of all cases satisfies the respective criterion for strongly ionized plasmas:

$$\nu_{jn} \ll \nu_{ei} \frac{m_e}{m_j} \frac{T_e + T_i}{T_j} \quad , \qquad j = e, i$$

For cases 3 to 5, therefore, we have calculated the diffusion coefficients for weakly as well as for strongly ionized plasmas from Kovrizhnik's theory (Appendix II.D).

For weakly ionized plasmas the following expressions are found:

$$D_K^A = \begin{cases} 4 \cdot \rho_e^2 \frac{\nu_e}{R_o \cdot t} \cdot c_e & 1 \ll c_e \\ 3{,}25 \cdot \rho_e^2 \frac{\nu_e}{R_o \cdot t} \left(1 + c_e\right) & \frac{1}{2}\left(\frac{r_o}{R_o}\right)^{1/2} < c < 1 \\ 14 \cdot \rho_e^2 \frac{\nu_e}{R_o \cdot t} \cdot c_e & c_e \ll \frac{1}{2}\left(\frac{r_o}{R_o}\right)^{1/2} \end{cases}$$

$$\left(\text{for } \frac{R_o}{r_o} = 10\right)$$

where c_e is mainly determined by electron neutral collisions.

For strongly ionized plasmas the following expressions apply:

$$D_K^A = \begin{cases} 0{,}69 \cdot \varrho_e^2 \frac{\nu_e}{R_0 t} \cdot c_e = 22{,}1 \cdot D_B \cdot \frac{\varrho_e}{R_0 t} \cdot c_e & 1 \ll c_e \\ 1{,}56 \cdot \varrho_e^2 \frac{\nu_e}{R_0 t} \left(\frac{1}{1 + 0{,}86 \cdot T_e^{3/2}} \right) & \frac{1}{2}\left(\frac{r_0}{R_0}\right)^{3/2} < c_e < 1 \end{cases}$$

$$= 50 \cdot D_B \frac{\varrho_e}{R_0 t} \left(\frac{1}{1 + 0{,}86 \cdot T_e} \right)$$

(for $\frac{R_0}{r_0} = 10$, T_e in eV)

Here, c_e includes electron ion and electron neutral collisions. Inserting $R_0 = 50$ cm and the respective numbers for B_0, t, T_e and n_{e0}, one can draw the curves of D vs. c_e for every discharge listed in Table I. An example is shown by Fig. 3 for case 3. From this procedure, and referring to the peak values of T_e and n_e, respectively, the values D_K^A are obtained and listed in Table I. c_e ranges from $1/14$ to 2. The values of D_K^A for strongly ionized plasmas lie close to the Pfirsch-Schlüter value, D_{PS}, for the plasmas considered in Table I. The last column of Table I contains the Bohm diffusion coefficient, D_B.

A comparison between the effective diffusion coefficients which are computed from the experimentally determined average life times τ by the relation $D_{eff} = (\frac{r_0}{2,4})^2 \cdot \frac{1}{\tau}$, shows that D_{eff} is generally between one to two orders of magnitude larger than D_A^K, but lies within a factor of ten below the Bohm value. In this comparison we have excluded case 6 which had an anomalously small average life time.

C. Photo-ionized Barium Plasma, $T_e \gg T_i$

As mentioned previously, with a photo-ionized plasma flux of 10^{11} particles per second a peak particle density of $1{,}3 \cdot 10^7$ cm^{-3} has been reached for $t \geq 0{,}1$ and 5 kilogauss main magnetic field. The electron and ion temperature are determined by the mechanism of photo-ionization and are estimated as $T_e \approx 1$ eV and $T_i \approx 0{,}1$ eV. The base pressure during this measurement was $7 \cdot 10^{-6}$ torr. Assuming air as rest gas and taking the relevant cross-sections,

the conditions for a weakly ionized plasma are fulfilled and c_e is in that range where the "plateau" value of the neoclassical diffusion coefficient:

$$D_K^A = 3{,}25 \cdot \varrho_e^2 \frac{v_e}{R_o \cdot t}$$

applies. Inserting figures, one finds $D_K^A = 17{,}6\ cm^2\,s^{-1}$ for $t = 0{,}1$ and $8{,}8\ cm^2\,s^{-1}$ for $t = 0{,}2$.

For comparison with the observed results the diffusion equation in cylindrical geometry is solved in Appendix III with a diffusion coefficient that is independent of n_e and r.

Assuming a cylindrical "source region" of 1 cm radius and inserting the measured values in the computed flux-density relation, one finds a diffusion coefficient of $8{,}1\ cm^2\,s^{-1}$ in good agreement with the theoretical estimate.

8. Diffusion in Non-Axisymmetric Systems

The helical stabilizing fields in a stellarator cause a modulation of the main magnetic field strength around the major axis. This modulation affects particles with very low $v_{\parallel}$ in such a way that they are trapped in the "helical mirrors". Numerical calculations of particle trajectories have shown that these "localized particles" can drift out of the confinement volume no matter how strong the field, they form a loss region in velocity space.[19] Localized particle diffusion occurs if the time between collisions is longer than the transit time between mirrors. For densities usually considered, this condition is only satisfied at high temperatures. It can be converted into a condition on c which reads:

$$c < \frac{p}{2\pi \cdot t} \cdot \left(\frac{2\alpha}{\pi}\right)^2$$

where p = number of helical field periods on the torus, and $\alpha^2 = \frac{B_{max} - B_{min}}{B_{min}}$

In W IIa the right hand side of the above inequality amounts to about 10^{-3}. The magnitudes of c in the present experiments are much larger.

Hence, localized diffusion should not occur according to this single particle picture.

The diffusion in stellarator magnetic fields has also been treated by Kovrizhnik. His assumptions, however, are not realistic for present day stellarators because they imply that the variations in main field strength due to the helical fields are stronger than those from toroidicity, i.e. from the radial variation of the main field. It is interesting to note, however, that in the case of very strong helical fields, ions and electrons diffuse at rates proportional to their own total collision frequency. Thus even in a fully ionized plasma ambipolar electric fields should arise.

It appears - even in the absence of an adequate theory - that for the experiments under discussion the effects of toroidicity play the dominant part. Nevertheless, we have evaluated the diffusion coefficient, D_K^S, in a stellarator from Kovrizhnik's theory for the ECR-generated plasmas, $T_e \gg T_i$ (see Appendix IV):

$$D_K^S = 16{,}4 \cdot \sqrt[4]{t} \cdot \left(\frac{r_o}{R_o}\right)^3 \cdot \frac{T_e}{T_i}\, \nu_i \cdot \rho_i^2 \, \frac{v_i^2}{v_E^2 + \nu_i^2 \cdot r_o^2}$$

$$= 525 \sqrt[4]{t^5} \left(\frac{r_o}{R_o}\right)^3 \cdot D_B \cdot \frac{\rho_i'}{R_o} \, \frac{c_i}{v_E^2/v_i^2 + r_o^2/(R_o t^{-1})^2 \cdot c_i^2}$$

where: $c_i = c_{ii} + c_{ie} + c_{io}$

$$v_E = \frac{3 \cdot \varkappa \cdot T_e}{\xi \cdot e \cdot B_o} \quad , \quad \xi = -\left(\frac{d\,(\ln n)}{dr}\right)^{-1}$$

After inserting $\left(\frac{r_o}{R_o}\right) = 10^{-1}$, $\xi \approx 3$ cm, the values of D_K^S in column 10 of Table I have been computed. They are comparatively small as a result of the strong dependence on r_o/R_o. They are certainly much less - for the range of parameters considered - than the diffusion coefficients which re-

sult from the inhomogeneity of the main field, as derived in the foregoing chapter.

9. Scaling of "Neoclassical" Diffusion

The extension of the plasma parameters presently available in the W IIa experiments towards higher temperatures, densities and magnetic fields has obvious importance. In order to get an idea about cross field diffusion during this extension, the diffusion coefficient in a fully ionized axisymmetric hydrogen plasma in the range of densities and electron temperatures, 10^{10} to 10^{13} cm^{-3} and 1-1000 eV, respectively, has been evaluated from Kovrizhnik's theory in Appendix III.C. The ion temperature was assumed to be one tenth of the electron temperature. The normalized diffusion coefficient can be expressed as a function of the normalized quantity $c_{ei} = \frac{R_o}{\lambda_{ei} \cdot t}$ as follows:

$$\frac{D_K^A}{D_B \cdot \frac{g_e}{R_o \cdot t}} \begin{cases} 24{,}3 \cdot c_{ei} & 1 \ll c_{ei} \\ 55 & \frac{1}{2}\left(\frac{r_o}{R_o}\right)^{3/2} < c_{ei} < 1 \\ 118{,}8 \cdot \left(\frac{R_o}{r_o}\right)^{3/2} \cdot c_{ei} & c_{ei} \ll \frac{1}{2}\left(\frac{r_o}{R_o}\right)^{3/2} \end{cases}$$

By choosing $R_o \cdot t = 10$, $R_o = 10 \cdot r_o$, $\frac{R_o}{t} = 10^3$, the product $(D \cdot B^2)$ is computed. Fig. 4 shows its dependence on electron temperature for various densities. In general, the diffusion coefficient rises with increasing density as would be expected for collisional diffusion. On the other hand, the very existence of the plateau value and its occurence in the region of parameter space under consideration, has some interesting consequences. For example, a relative minimum shows up in each D vs. T_e-curve for given density. These minima occur in that region of the D-T_e-plane where the Pfirsch-Schlüter coefficient (valid at low temperatures) changes over into the neoclassical plateau which is independent of density but increases as $T_e^{3/2}$. The minima will probably be more pronounced when considering that at low temperatures the plasma is

not fully ionized and ambipolar effects increase cross field diffusion. When extrapolating the densities and temperatures at these relative minima towards lower values one arrives in the vicinity of the present contact ionization regime. The magnitude of $(D \cdot B)^2$ at the relative minima is a steep function of electron temperature, as may be already seen from Fig. 4, and scales roughly as $n^{0.8}$ with density.

Hence, any extension of plasma parameters from those in the contact ionization regime or from those characterizing a typical preionization plasma with a temperature of several electronvolts towards higher densities and temperatures, is inevitably connected with an increase in particle diffusion x). This should be borne in mind when future experiments are planned on the basis of the experiments with contact ionized plasmas. In view of the high costs involved, the time scale of such experiments should be derived from the conditions for achieving higher densities and temperatures, i.e., the rate of heating power input and the equipartition times of electron and ion energies, rather than by the demands for steady state operation. Studying these conditions requires insight into the energy balance on the basis of neoclassical transport theory with due allowance of anomalous effects.

10. Acknowledgements

I would like to thank Drs. R.A. Ellis, Jr. and G.v. Gierke for many helpful comments.

---

x) The influence of cross field diffusion caused by fluctuations which eventually might appear, is neglected.

Table I: Diffusion coefficients of ECR-generated argon plasmas

No	W [watts]	B_o [Kgauss]	n_{eo} [cm^{-3}]	$\dot{N}$ [sec^{-1}]	τ	D_{eff}	D_{PS}	D_K^A	D_K^S	D_B
	p [torr]	τ	T_{eo} [eV]		[msec]	[$cm^2\,sec^{-1}$]	[$cm^2\,sec^{-1}$]	[$cm^2\,sec^{-1}$]	[$cm^2\,sec^{-1}$]	[$cm^2\,sec^{-1}$]
1	0,04	3,2	$3,8x10^8$	$1,3x10^{15}$	1	$4,3x10^3$	0,43	$0,58x10^3$	1,32	$16,8x10^3$
	$6x10^{-6}$	0,125	8,6	$2,5x10^{15}$	0,5	$8,6x10^3$				
2	0,04	3,2	$9x10^8$		2,9	$1,5x10^3$	0,273	$0,058x10^3$	3,48	$13,3x10^3$
	$8x10^{-6}$	0,253	6,8							
3	0,4	4,62	$6,3x10^9$	$4,8x10^{16}$	0,79	$5,5x10^3$	1,36	$0,11x10^3$	0,78	$10x10^3$
	$7x10^{-6}$	0,2	7,4	$2,5x10^{16}$	1,5	$2,9x10^3$		$0,007x10^3$		
4	7	3,28	$2,4x10^{11}$	$1,6x10^{18}$	0,3	$14,5x10^3$	32	$0,5x10^3$	0,074	$23x10^3$
	$4,6x10^{-6}$	0,328	12	$0,5x10^{18}$	1	$4,5x10^3$		$0,043x10^3$		
5	7	3,28	$1,5x10^{11}$	$2,2x10^{18}$	0,3	$14,5x10^3$	52	$0,64x10^3$	0,079	$18,4x10^3$
	$9x10^{-6}$	0,2	9,6	$0,5x10^{18}$	1,3	$3,3x10^3$		$0,06x10^3$		
6	0,4	4,62	$2x10^9$	$1x10^{16}$	0,1	$43,2x10^3$	0,56	$0,24x10^3$	1,35	$6x10^3$
	$2x10^{-4}$	0,2	4,4	$2,5x10^{16}$	0,04	$133x10^3$				

Appendix I

Determination of the Effective Diffusion Coefficient from the Observed Φ vs. n-Dependence

In steady state the total imput flux, Φ, is equal to the recombination flux to the emitter and the cross field loss flux both being proportional to the square of peak particle density n_{eo} in the absence of probes (and emitter supports):

$$\Phi_{th} = R \cdot n_{eo}^2 + A_{th} \cdot \alpha_{th} \cdot n_{eo}^2$$

where A is the diffusion coefficient divided by the density and α is a numerical factor depending on geometry. The experiments show a similar $\Phi \propto n_{eo}^2$-relation:

$$\Phi_{exp} = R \cdot n_{eo}^2 + A_{exp} \cdot \alpha_{exp} \cdot n_{eo}^2$$

From these relations follows:

$$A_{exp} = A_{th} \frac{\Phi_{exp} - R \cdot n_{eo}^2}{\Phi_{th} - R \cdot n_{eo}^2} \quad , \quad \alpha_{exp} \approx \alpha_{th}$$

Taking the measurements of Fig. 5 in Ref. 6 [x] for $n_{eo} = 10^9\ cm^{-3}$:
$\Phi_{exp} = 5 \times 10^{12}\ s^{-1}$, $\Phi_{th} = 1{,}5 \times 10^{12}\ s^{-1}$ (at $T_e = 0{,}18$ eV) and $\Phi_{th} = 8{,}4 \times 10^{11}\ s^{-1}$ (at $T_e = 0{,}2$ eV) and computing the recombination fluxes from:

$67{,}5 \cdot 10^{-8} (10^9)^2 = 6{,}75 \cdot 10^{11}\ s^{-1}$ at $T_e = 0{,}18$ eV

$5 \cdot 10^{-8} (10^9)^2 = 5 \cdot 10^{10}\ s^{-1}$ at $T_e = 0{,}2$ eV

one gets:

$$\frac{A_{exp}}{A_{th}} = \begin{cases} 5{,}24 & (0{,}18\ eV) \\ 6{,}26 & (0{,}2\ eV) \end{cases}$$

---

x) After improving the stabilization of the currents through the helical windings, somewhat higher peak densities have been observed.

With $D_{th} = \frac{3{,}55 \cdot 10^{-3} \cdot \ln\Lambda \cdot n}{t^2 \cdot T_e \cdot B_o^2}$ $cm^2\,s^{-1}$, B_o in gauss, T_e in ^oK

one obtains at $n_{eo} = 10^9\,cm^{-3}$, $B_o = 5$ kgauss, $t = 0{,}1$

$$D_{exp} = \begin{cases} 16{,}3\ cm^2\,s^{-1} & (0{,}18\ eV) \\ 18{,}5\ cm^2\,s^{-1} & (0{,}2\ eV) \end{cases}$$

Appendix II

Evaluation of the Diffusion Coefficient D_K^A for Axisymmetric Plasmas from the Theory of Kovrizhnik

A. Barium Plasma, $T_e = T_i$.

The condition for a strongly ionized plasma (Kovrizhnik, eq. 14)

$$\nu_{jn} \ll \frac{m_e}{m_j}\,\nu_{ei}\,\frac{T_e + T_i}{T_j} \quad , \quad j = e, i$$

is for electrons:

$$\nu_{en} \ll 2\,\nu_{ei}$$

Taking air as rest gas at a pressure of 10^{-6} torr and using the following cross-sections for electrons (in $10^{-16}\ cm^2$):[18]

	N_2	O_2	average
0,2 eV	8,0	3,1	5,5
2 eV	24	6,6	15,5
20 eV	12	(10)	11

and $\nu_{ei} = 4{,}2 \cdot 10^{-4} \cdot n_e$ (for 0,2 eV) with $n_e = 3 \cdot 10^8 \ldots 5 \cdot 10^9\,cm^{-3}$, the above criterion is fully satisfied at low electron temperatures and marginally at $T_e = 20$ eV.

For ions:

$$\nu_{in} \ll 2\,\frac{m_e}{m_i}\,\nu_{ei}$$

If we take $Q \approx 60 \cdot 10^{-16}\,cm^2$ as collision cross-section of the Ba^+-ions with the rest gas atoms, [20] the above criterion is only marginally satisfied. Within the accuracy of this estimate we, nevertheless, take Kovrizhnik's equation for a strongly ionized plasma (eq. 15) and set $\frac{\partial \ln n_j}{\partial r} = \frac{\partial \ln T_j}{\partial r}$ for simplicity.

$$S_r^e = S_r^i = -\nu_{ei}\,\frac{2\pi^2}{\iota^2 m_e \cdot \omega_e^2}\left[\frac{1}{\frac{\nu_{ie}}{\nu_i}\,\frac{1}{\hat{q}_2(c_i)} + \frac{\nu_{ei}}{\nu_e}\,\frac{1}{\hat{q}_2(c_e)}}\right]\cdot\Bigg[$$

$$\left[T_e\left\{1+\frac{\hat{q}_3(c_i)}{\hat{q}_2(c_i)}-\frac{3}{2}\right\}+T_i\left\{1+\frac{\hat{q}_3(c_e)}{\hat{q}_2(c_e)}-\frac{3}{2}\right\}\right]\cdot\frac{\partial n_e}{\partial r}$$

where $c_j = \frac{\nu_j}{v_j}\,\frac{R_0}{t}$

With $D = -\frac{S_r^e}{\frac{\partial n_e}{\partial r}}$ and $T_e = T_i$, we have

$$D = \nu_{ei}\,\frac{2\pi^2 \cdot T_e}{\iota^2 m_e \omega_e^2}\left[\frac{1}{\frac{\nu_{ie}}{\nu_i}\,\frac{1}{\hat{q}_2(c_i)} + \frac{\nu_{ei}}{\nu_e}\,\frac{1}{\hat{q}_2(c_e)}}\right]\left[\frac{\hat{q}_3(c_e)}{\hat{q}_2(c_e)} + \frac{\hat{q}_3(c_i)}{\hat{q}_2(c_i)} - 1\right]$$

where the functions $\hat{q}_s(c_j)$ are declared for specific ranges of c_j.

We consider the second square bracket and notice from Kovrizhnik (eq. 17) that $\frac{\hat{q}_3(c_j)}{\hat{q}_2(c_j)}$ can assume either $\frac{3!}{2!} = 3$ or $\frac{2{,}5!}{1{,}5!} = 2{,}77$.
Hence, we may set the second square bracket equal to 5.

The denominator of the first square bracket reads:

$$\frac{\nu_{ei}}{\nu_e}\,\frac{1}{\hat{q}_2(c_e)}\cdot\left(1+\frac{\nu_{ie}}{\nu_{ei}}\,\frac{\nu_e}{\nu_i}\,\frac{\hat{q}_2(c_e)}{\hat{q}_2(c_i)}\right)$$

Now: $\frac{\nu_{ie}}{\nu_{ei}} \approx \frac{m_e}{m_i} = 4 \cdot 10^{-6}$ (for barium). ν_i will be mainly determined by ion-neutral collisions under the conditions assumed above. Hence c_i is in the range where $\hat{q}_2(c_i) = \frac{\sqrt{2\pi}}{c_i}$

Thus

$$\frac{\nu_{ei}}{\nu_e}\ \frac{1}{\hat{q}_2(c_e)}\left(1+\ \frac{4\cdot 10^{-6}}{\sqrt{2\pi}}\ \frac{v_e}{v_i}\cdot c_e\cdot \hat{q}_2(c_e)\right)\cdot$$

$$=\ \frac{\nu_{ei}}{\nu_e}\ \frac{1}{\hat{q}_2(c_e)}\left(1+\ 8\cdot 10^{-4}\cdot c_e\cdot \hat{q}_2(c_e)\right)$$

Now $c_e\cdot\hat{q}_2(c_e)$ is either equal to $\sqrt{2\pi}$ or less than $(c_e)_{max}\cdot\hat{q}_2(c_e) = \sqrt{2\pi}\cdot 2{,}5$!

Thus the first square bracket becomes

$$\left(\frac{\nu_{ei}}{\nu_e}\ \frac{1}{\hat{q}_2(c_e)}\right)^{-1}$$

Hence

$$D = \frac{2\pi^2\cdot T_e\cdot 5}{\iota^2 m_e w_e^2}\cdot \nu_e\cdot \hat{q}_2(c_e) = 2{,}5\cdot\frac{T_e}{m_e\cdot w_e^2}\cdot\frac{v_e}{R_0\cdot t}\cdot c_e\cdot\hat{q}_2(c_e)$$

$$= 40\cdot D_B\cdot\frac{\varrho_e}{R_0 t}\cdot c_e\cdot\hat{q}_2(c_e) \qquad \varrho_e = \text{electron Larmor radius}$$

For $c_{ei} \ll \left(\frac{r_0}{R_0}\right)^{3/2}$:

$$D = 126\cdot D_B\cdot\frac{\varrho_e}{R_0 t}\left(\frac{R_0}{r_0}\right)^{3/2}\cdot c_e = 216\cdot D_B\frac{\varrho_e}{R_0 t}\left(\frac{R_0}{r_0}\right)^{3/2}\cdot c_{ei}$$

for $\left(\frac{r_0}{R_0}\right)^{3/2} < c_{ei} < 1$:

$$D = 100\cdot D_B\cdot\frac{\varrho_e}{R_0 t}$$

For c_e, $c_i \gg 1$, the hydrodynamic approximation is valid:

$$v_\perp = -\frac{1}{t^2}\ \frac{\eta_\perp}{B^2}\cdot\nabla p = -D\cdot\frac{\nabla n}{n}$$

$$D = 4\ \frac{\eta_\perp\, n\, k T}{t^2\cdot B^2}\ ,\quad \frac{\nabla n}{n} = \frac{\nabla(T_e+T_i)}{T_e+T_i}\ ,\quad T_e = T_i$$

$$\left.\begin{aligned} \eta_\perp &= \frac{1{,}29 \cdot 10^4 \cdot \ln\Lambda}{T_e^{\,3/2}} \\ \tau_{ei} &= \frac{0{,}714 \cdot 0{,}266 \cdot T_e^{\,3/2}}{n_e \cdot \ln\Lambda} \end{aligned}\right\} \quad T_e \text{ in } {}^\circ K,\ n_e \text{ in } cm^{-3}$$

Thus, for $c_{ei} \gg 1$

$$D = \frac{1{,}38 \cdot \varrho_e^2 \cdot \nu_{ei}}{t^2} = 1{,}38 \cdot \varrho_e^2 \frac{\nu_e}{R_o \cdot t} \cdot c_{ei} = 44{,}2 \cdot D_B \frac{\varrho_e}{R_o \cdot t} \cdot c_{ei}$$

B. Strongly Ionized Argon Plasma, $T_e \gg T_i \approx 1/40$ ev.

In this case we only need the plateau value for $\left(\tau/R_o\right)^{3/2} < c_e < 1$ and assume for simplicity that c_i is in the same range. The denominator of the first square bracket in the expression for S_r^j becomes then:

$$\frac{\nu_{ei}}{\nu_e} \frac{c_e}{\sqrt{2\pi}} \left(1 + \frac{\nu_{ie}}{\nu_{ei}} \frac{\nu_e}{\nu_i} \frac{c_i}{c_e}\right) = \frac{\nu_{ei}}{\nu_e} \frac{c_e}{\sqrt{2\pi}} \left(1 + \frac{\nu_{ie}}{\nu_{ii}} \frac{\lambda_{ee}}{\lambda_{ii}} \frac{\nu_{ee}}{\nu_{ei}}\right)$$

with

$$\frac{\lambda_{ee}}{\lambda_{ii}} = \left(\frac{T_e}{T_i}\right)^2$$

$$\frac{\nu_{ie}}{\nu_{ii}} = \left(\frac{m_e}{m_i} \frac{T_i}{T_e}\right)^{1/2} \frac{0{,}92}{0{,}714}$$

$$\frac{\nu_{ee}}{\nu_{ei}} = 0{,}714$$

one gets

$$\frac{\nu_{ei}}{\nu_e} \frac{c_e}{\sqrt{2\pi}} \left(1 + 0{,}86 \cdot T_e^{\,3/2}\right) \quad \text{with } T_e \text{ in eV.}$$

The second square bracket reduces to $2{,}5 \cdot T_e$.

We then obtain

$$D = \nu_{ei} \frac{2\pi^2}{L^2 \cdot m_e \cdot \omega_e^2} \cdot 2{,}5 \cdot T_e \frac{\sqrt{2\pi} \cdot v_e \cdot t}{\nu_{ei} \cdot R_o \left(1 + 0{,}86 \cdot T_e^{3/2}\right)}$$

$$= 1{,}56 \cdot \varrho_e^2 \frac{v_e}{R_o \cdot t} \frac{1}{\left(1 + 0{,}86 \cdot T_e^{3/2}\right)}$$

$$= 50 \cdot D_B \cdot \frac{\varrho_e}{R_o \cdot t} \frac{1}{\left(1 + 0{,}86 \cdot T_e^{3/2}\right)}$$

For the hydromagnetic range, $c_e \gg 1$, we get - with $T_i \ll T_e$ - half the value deduced for an isothermal plasma in Part A, i.e.:

$$D = 0{,}69 \cdot \frac{\varrho_e^2 \cdot \nu_{ei}}{t^2} = 0{,}69 \cdot \varrho_e^2 \frac{v_e \cdot c_e}{R_o \cdot t} = 22{,}1 \cdot D_B \frac{\varrho_e}{R_o \cdot t} \cdot c_e$$

C. Fully Ionized Hydrogen Plasma, $T_e = 10 \cdot T_i$.

The denominator in the first square bracket is:

$$\frac{\nu_{ei}}{\nu_e} \frac{1}{\hat{q}_2(c_e)} \left(1 + \frac{\nu_{ie}}{\nu_{ei}} \frac{v_e}{v_i} \frac{\hat{q}_2(c_e)}{\hat{q}_2(c_i)}\right)$$

with:

$$\nu_i \approx \nu_{ii}$$

$$\nu_e = \nu_{ei} + \nu_{ee} = 2{,}4 \cdot \nu_{ee} = 1{,}71\, \nu_{ei}$$

$$c_i = \frac{c_i}{c_e} \cdot c_e = \frac{\nu_{ii}}{2{,}4 \cdot \nu_{ee}} \cdot \frac{v_e}{v_i} \cdot c_e = \frac{1}{2{,}4} \left(\frac{T_e}{T_i}\right)^2 \cdot c_e = 42 \cdot c_e$$

$$\nu_{ii} \approx \left(\frac{m_e}{m_i} \frac{T_e}{T_i}\right)^{1/2} \cdot \nu_{ie}$$

$$\frac{\nu_{ei}}{\nu_e} \frac{1}{\hat{q}_2(c_e)} \left(1 + 10^{-2} \frac{\hat{q}_2(c_e)}{\hat{q}_2(c_i)}\right)$$

The maximum value which $\frac{\hat{q}_2(c_e)}{\hat{q}_2(c_i)}$ can assume is $\approx \left(R_0/r_0\right)^{3/2} = 31{,}6$. Thus we may drop the second term in the above round brackets. In this case, we get the same expressions for D as derived in Part A except for a numerical constant that stands for the different ratios of electron and ion temperatures.

D. Weakly Ionized Argon Plasma, $T_e \gg T_i = 1/40\,\text{eV}$

The radial particle fluxes have the form (Kovrizhnik, eq. 11):

$$S_r^j = -A_j \left\{ \left(3 + q_2^j + q_1^j \cdot c_j^2\right)\left(\frac{\partial \ln n_j}{\partial r} - \frac{e_j \cdot E_r}{T_j}\right) + \left(4 + q_3^j - \frac{3}{2} q_2^j\right) \frac{\partial \ln T_j}{\partial r} \right\}$$

where $A_j = \nu_{jn} \cdot n_j \frac{2\pi^2}{L^2} \cdot \varrho_j^2$, $\quad j = e, i$

ϱ_j = Larmor radius

$c_j = \frac{\nu_j}{v_j} \frac{R_0}{r}$

q_s^j are functions of c_j declared for specific ranges of c_j. As the ions are cold, c_j is $\gg 1$, but c_e of the electrons can assume different values depending on density and electron temperature. We assume generally $\frac{\partial \ln n_j}{\partial r} = \frac{\partial \ln T_j}{\partial r} = -\frac{1}{\xi}$.

For $c_e \ll \frac{1}{2}\left(\frac{r_0}{R_0}\right)^{1/2} \approx \frac{1}{2} \cdot \frac{1}{\sqrt{10}}$

$$S_r^e = A_e \left(\frac{28}{\xi} - 13{,}5 \cdot \frac{e \cdot E_r}{T_e}\right)$$

$$S_r^i = A_i \left(\frac{8}{\xi} + 4\,\frac{e \cdot E_r}{T_i}\right)$$

Hence $e \cdot E_r = \frac{1}{\xi} \cdot T_e \cdot \frac{28}{13{,}5} \cdot \frac{1 - \frac{8}{28}\frac{A_i}{A_e}}{1 + \frac{4}{13{,}5}\frac{A_i}{A_e}\frac{T_e}{T_i}}$

and

$$S_r^e = A_e \cdot \frac{28}{\xi}\left(1 - \frac{1 - \frac{8}{28}\frac{A_i}{A_e}}{1 + \frac{4}{13{,}5}\frac{A_i}{A_e}\frac{T_e}{T_i}}\right)$$

In the denominator of the second term in the round brackets:

$$\frac{A_i}{A_e}\frac{T_e}{T_i} = \frac{\nu_{in}}{\nu_{en}} \cdot \frac{m_i}{m_e}$$

is usually large compared with unity ($\approx 10^2$). Hence

$$S_r^e = A_e \cdot \frac{28}{\xi}\left(1 + \frac{T_i}{T_e}\right) \approx A_e \cdot \frac{28}{\xi}$$

and

$$D = \frac{S_r^e \cdot \xi}{n} = \nu_{en} \cdot \frac{2\pi^2}{l^2}\varrho_e^2 \cdot 28 = 14 \cdot \varrho_e^2 \frac{v_e}{R_0 \cdot t} \cdot c_e$$

For $\frac{1}{2}\left(\frac{r_0}{R_0}\right)^{1/2} < c_e < 1$

$$S_r^e = A_e\left\{\left(7 + 5\cdot\sqrt{\frac{\pi}{2}}\cdot\frac{1}{c_e} + \sqrt{\frac{\pi}{2}}\cdot c_e\right)\cdot\frac{1}{\xi} - \left(3 + 2\cdot\sqrt{\frac{\pi}{2}}\cdot\frac{1}{c_e} + \sqrt{\frac{\pi}{2}}\cdot c_e\right)\frac{e\cdot E_r}{T_e}\right\}$$

$$= A_e\left\{a\cdot\frac{1}{\xi} - b\cdot\frac{e\cdot E_r}{T_e}\right\}$$

$$S_r^i = A_i\left\{\frac{8}{\xi} + 4\cdot\frac{e\cdot E_r}{T_i}\right\}$$

Hence

$$e\cdot E_r = \frac{T_e}{\xi}\cdot\frac{a}{b}\,\frac{1 - \frac{8}{a}\cdot\frac{A_i}{A_e}}{1 + \frac{4}{b}\frac{A_i}{A_e}\frac{T_e}{T_i}}$$

and

$$S_r^e = A_e\frac{a}{\xi}\left(1 - \frac{1 - \frac{8}{a}\cdot\frac{A_i}{A_e}}{1 + \frac{4}{b}\cdot\frac{A_i}{A_e}\cdot\frac{T_e}{T_i}}\right) \approx A_e\frac{a}{\xi}\left(1 + 2\frac{b}{a}\frac{T_i}{T_e}\right)$$

as the denominator in the second term of the round bracket is usually large in our cases. Thus

$$D = \frac{S_r^e \cdot \xi}{n} = \nu_{en} \frac{2\pi^2}{L^2} \rho_e^2 \left(7 + \frac{6{,}5}{c_e} + 1{,}25 \cdot c_e\right) \cdot O(1)$$

$$= \frac{v_e}{R_o} \frac{\pi}{L} \rho_e^2 \, 6{,}5 \left(1 + \frac{7}{6{,}5} \cdot c_e + 1{,}25 c_e^2\right) \cdot O(1)$$

$$\approx 3{,}25 \, \rho_e^2 \frac{v_e}{R_o t} \left(1 + c_e\right)$$

For $c_e \gg 1$

$$S_r^e = A_e \left(\frac{\delta}{\xi} - \frac{4e \cdot E_r}{T_e}\right)$$

$$S_r^i = A_i \left(\frac{\delta}{\xi} + \frac{4e \cdot E_r}{T_i}\right)$$

hence

$$e \cdot E_r = \frac{2}{\xi} T_e \frac{1 - \frac{A_i}{A_e}}{1 + \frac{A_i}{A_e} \cdot \frac{T_e}{T_i}} \approx -\frac{2}{\xi} T_i$$

and

$$S_r^e = A_e \cdot \frac{\delta}{\xi} \left(1 + \frac{T_i}{T_e}\right) \approx A_e \cdot \frac{\delta}{\xi}$$

$$D = \frac{S_r^e \cdot \xi}{n} = \nu_{en} \frac{16\pi^2}{L^2} \rho_e^2 = 4 \cdot \rho_e^2 \frac{v_e}{R_o \cdot t} \cdot c_e$$

Appendix III

Diffusion in a Straight Plasma Cylinder with a Constant Diffusion Coefficient D

Inside the source region:

$$\frac{1}{r}\cdot\frac{d}{dr}\left(r\cdot n\cdot v_r\right)=\mu = \text{constant production rate}$$

$$n\cdot v_r = -D\frac{dn}{dr}$$

$$\frac{1}{r}\frac{d}{dr}\left(-r\frac{dn}{dr}\right)=\frac{\mu}{D}$$

$$n = C_1 - \frac{\mu}{D}\frac{r^2}{4}$$

for r = O, n = n_o: $$\frac{n}{n_o} = 1 - \frac{\mu}{D\cdot n_o}\frac{r^4}{4}$$

Outside the source region:

$$\frac{d}{dr}\left(r\cdot\frac{dn}{dr}\right)=0$$

$$n = C_2 \ln\frac{r_w}{r}$$ with n = O at wall radius r_w.

Matching the two solutions at the boundary of the source region, r = r_Q:

$$n(r_Q) = n_o - \frac{\mu}{D}\frac{r_Q^2}{4} = C_2 \ln\frac{r_w}{r_Q}$$

$$\left.\frac{dn}{dr}\right|_{r_Q} = -\frac{\mu}{D}\frac{r_Q}{2} = -\frac{C_2}{r_Q}$$

gives: $$C_2 = \frac{\mu\cdot r_Q^2}{2D}, \qquad n_o = \frac{\mu}{D}\frac{r_Q^2}{4}\left(1+2\ln\frac{r_w}{r_Q}\right)$$

A relation between production rate μ and the total input flux Φ from the total outward flux at the boundary r = r_Q can be established:

$$-D\left.\frac{dn}{dr}\right|_{r_Q} = \frac{\mu\cdot r_Q}{2}$$

$$-2\pi R_o\cdot 2\pi r_Q\cdot D\left.\frac{dn}{dr}\right|_{r_Q} = 2\pi R_o\,\pi r_Q^2\cdot\mu = \Phi$$

$$\Phi = \frac{2\pi R_0 \, 4\pi D \cdot n_0}{1 + 2 \ln \frac{r_w}{r_Q}}$$

Hence

$$D = \frac{\Phi}{n_0} \frac{1 + 2 \ln \frac{r_w}{r_Q}}{8\pi^2 \cdot R_0}$$

Inserting $\Phi = 10^{11}$ sec^{-1}, $n_0 = 1{,}3 \cdot 10^7$ cm^{-3}, $R_0 = 50$ cm, $r_w = 5$ cm, $r_Q = 1$ cm, gives

$$D = \frac{10^{11} \cdot 4{,}12}{1{,}3 \cdot 10^7 \cdot 4 \cdot 10^3} = 8{,}1 \text{ cm}^2 \text{ s}^{-1}$$

Appendix IV

Evaluation of the Diffusion Coefficient in a Stellarator Field from the Theory of Kovrizhnik (ECR-Plasma, $T_i \ll T_e$)

The magnetic field in a stellarator with $\ell = 2$ is given by Kovrizhnik in the following form:

$$\vec{B} = \frac{\vec{e_\zeta} \cdot B_0}{1 + \frac{r}{R_0} \cdot \cos\varphi} + \vec{B}_1$$

$$\vec{B}_1 = \nabla\phi \quad , \quad \zeta = R_0 \cdot \theta$$

$$\phi = \frac{\varepsilon}{a} \cdot B_0 \cdot I_2(2ar) \cdot \sin\left[2\,(\varphi - a \cdot \zeta)\right]$$

with $a = \frac{2,5}{R_0}$ for the five helical periods in W IIa.

ε can be expressed by ι if we approximate $I_2(2\,ar) \approx \frac{1}{2!}\left(\frac{2\,ar}{2}\right)^2$:

$$\varepsilon = \sqrt{\frac{2}{5}\iota}$$

The criterion for a "sufficiently strong" radial electric field E_{r_0} (see eq. 23)

$$\left|\frac{e_j \cdot r_0 \cdot E_{r_0}}{T_j}\right| \gg \varepsilon \cdot 2 \cdot r_0 \frac{\partial}{\partial r_0}\left(I_2(2ar_0)\right) = \sqrt{\frac{2}{5}\iota} \cdot 2\left(\frac{2,5\,r_0}{R_0}\right)^2 \approx 4,5 \cdot 10^{-2}$$

is satisfied if we set $e \cdot E_{r_0} \approx \frac{T_e}{r_0}$

for electrons: $\frac{r_0}{T_e}\frac{T_e}{r_0} = 1$

and for ions: $\frac{r_0}{T_i} \cdot \frac{T_e}{r_0} = \frac{T_e}{T_i} \gg 1$

Hence the radial fluxes are (eqs. 21, 24):

$$S^e = -C \cdot A_e \left\{ \frac{\partial \ln n_e}{\partial r} + 2\,\frac{\partial \ln T_e}{\partial r} + \frac{e \cdot E_r}{T_e} \right\}$$

$$S^i = -C \cdot A_i \left\{ \frac{\partial \ln n_i}{\partial r} + 2 \frac{\partial \ln T_i}{\partial r} - \frac{e \cdot E_r}{T_i} \right\}$$

$$C = n \left(\frac{r}{R_0} \right)^2 \sqrt{\frac{4 \cdot \varepsilon \cdot I_2}{\pi}} \cdot 2{,}5 \; !$$

$$A_j = \nu_j \cdot \varrho_j^2 \frac{v_j^2}{v_E^2 + r^2 \cdot \nu_j^2} \quad , \quad j = e, i$$

ϱ_j = Larmor radius

$\nu_j = \nu_{ji} + \nu_{je} + \nu_{jo}$, $v_E = \frac{E_r}{B_o}$

With $\frac{\partial \ln n_j}{\partial r} = \frac{\partial \ln T_j}{\partial r} = -\frac{1}{\xi}$

and equalizing the loss fluxes, the electric field can be determined:

$$e \cdot E_r = \frac{3}{\xi} \cdot T_e \frac{1 - \frac{A_i}{A_e}}{1 + \frac{A_i}{A_e} \frac{T_e}{T_i}}$$

Now

$$\frac{A_i}{A_e} \frac{T_e}{T_i} = \frac{\nu_i \cdot T_i}{\nu_e \cdot T_e} \frac{v_E^2 + r_o^2 \nu_e^2}{v_E^2 + r_o^2 \nu_i^2} < 1$$

for our conditions and hence

$$\frac{A_i}{A_e} \ll 1$$

$$e \cdot E_r \approx \frac{3}{\xi} T_e \left(1 - \frac{A_i}{A_e} \frac{T_e}{T_i} \right)$$

we get:

$$S = C \cdot A_e \left\{ \frac{3}{\xi} - \frac{3}{\xi} \left(1 - \frac{A_i}{A_e} \frac{T_e}{T_i} \right) \right\} = \frac{3 C A_i}{\xi} \frac{T_e}{T_i}$$

$$= 3 \cdot 2{,}5! \cdot n \cdot \left(\frac{r}{R_0} \right)^2 \sqrt{\frac{4 \cdot \varepsilon \cdot I_2}{\pi}} \cdot \frac{T_e}{T_i} \cdot \nu_i \varrho_i^2 \cdot \frac{v_i^2}{v_E^2 + r^2 \cdot \nu_i^2} \left(- \frac{\partial \ln n}{\partial r} \right)$$

With $D_K^S = -\frac{S}{\frac{\partial n}{\partial r}}$

$$D_K^S\Big|_{r_0} = 3 \cdot 2{,}5! \left(\frac{r}{R_0}\right)^2 \sqrt{\frac{4}{\pi}\sqrt{\frac{2}{5}\cdot t}\cdot 2{,}5^2 \cdot \left(\frac{r_0}{R}\right)^2}\, \frac{T_e}{T_i}\, \frac{\nu_i \varrho_i^2 \cdot v_i^2}{v_E^2 + \tau^2 \nu_i^2}$$

$$= 16{,}4 \cdot \left(\frac{r_0}{R_0}\right)^3 \sqrt[4]{t}\; \frac{T_e}{T_i}\, \nu_i \varrho_i^2\, \frac{v_i^2}{v_E^2 + \tau_0^2 \nu_i^2} \quad , v_E \approx \frac{3 \cdot T_e}{\xi \cdot B_0 \cdot e}$$

References

1 L. Spitzer, Jr., Phys. Fluids 1

2 I.G. Brown et.al., Proceedings Novosibirsk Conf. IAEA (Vienna) 1969, Vol. I, p. 497

3 K.M. Young, Phys. Fluids 10 (1967) p. 213

4 A.A. Galeev, R.Z. Sagdeev, Soviet Physics JETP 26 (1968) p. 233

5 E. Berkl et al., Phys.Rev.Letts 17 (1966) p. 906

6 E. Berkl et al., Proceedings Novosibirsk Conf. IAEA (Vienna) 1969, Vol. I, p. 513

7 R.A. Ellis Jr., D. Eckhartt, IPP-Report 2/85 (1970)

8 L. Kovrizhnik, Soviet Physics JETP 29 (1969) p. 475

9 See, for example: H. Grad, Physics Today 22 (December 1969) p. 41

10 G.v. Gierke, 3rd European Conf.Contr.Fusion Plasma Physics, Utrecht (1969)

11 G. Grieger. Private communication

12 M.S. Beretshetskii et al., Proceedings Novosibirsk Conf. IAEA (Vienna) 1969, Vol. I, p. 529

13 S. Yoshikawa et al., Proceedings Novosibirsk Conf. IAEA (Vienna) 1969, Vol. I, p. 403

14 Annual Report 1969, Institut für Plasmaphysik GmbH, München-Garching, p. 32

15 G. Levine et al., MATT-Report, Princeton University, 479 (1966)

16 J.J. Thomson, G.P. Thomson, "The Conduction of Electricity through Gases". Dover Publ. Inc. New York (1969) Vol. II, p. 103

17 A.v. Engel, "Ionized Gases". Oxford University Press

18 J.L. Delcroix, "Plasma Physics". Vol. II. John Wiley a. Sons Ltd. London (1968).

19 A. Gibson, D.W. Mason, Plasma Physics, 11 (1969) p. 121

20 K.W. Michel, Max-Planck-Institut f. Extraterrestrische Physik. Private communication.

Figures

Fig. 1 The neoclassical diffusion coefficient D as a function of density at various temperatures for an axisymmetric fully ionized isothermal barium plasma (full curves) and with first order corrections for electron neutral collisions with the rest gas atoms (broken lines). The dotted lines represent the hydromagnetic (Pfirsch-Schlüter) diffusion coefficient. The hatched area denotes the experimentally observed values.

Fig. 2 The neoclassical diffusion coefficient D as a function of temperature for various densities for an axisymmetrie fully ionized isothermal barium plasma (full curves) and corrected for electron neutral collisions (broken lines). The dotted lines represent the hydromagnetic diffusion coefficient.

Fig. 3 The neoclassical diffusion coefficient D vs. c_e in an ECR-generated argon plasma (Case 3 of Table I). Also shown are the experimentally found values, D_{eff}, converted from the average plasma life time τ by the relation $D_{eff} = \left(\frac{r_o}{2,4}\right)^2 \cdot \frac{1}{\tau}$.

Fig. 4 The normalized diffusion coefficient $(D \cdot B^2)$ vs. electron temperature at various densities in a fully ionized axisymmetric hydrogen plasma. $R_o \cdot t = 10$, $\frac{R_o}{t} = 1000$, $\frac{R_o}{r_o} = 10$.

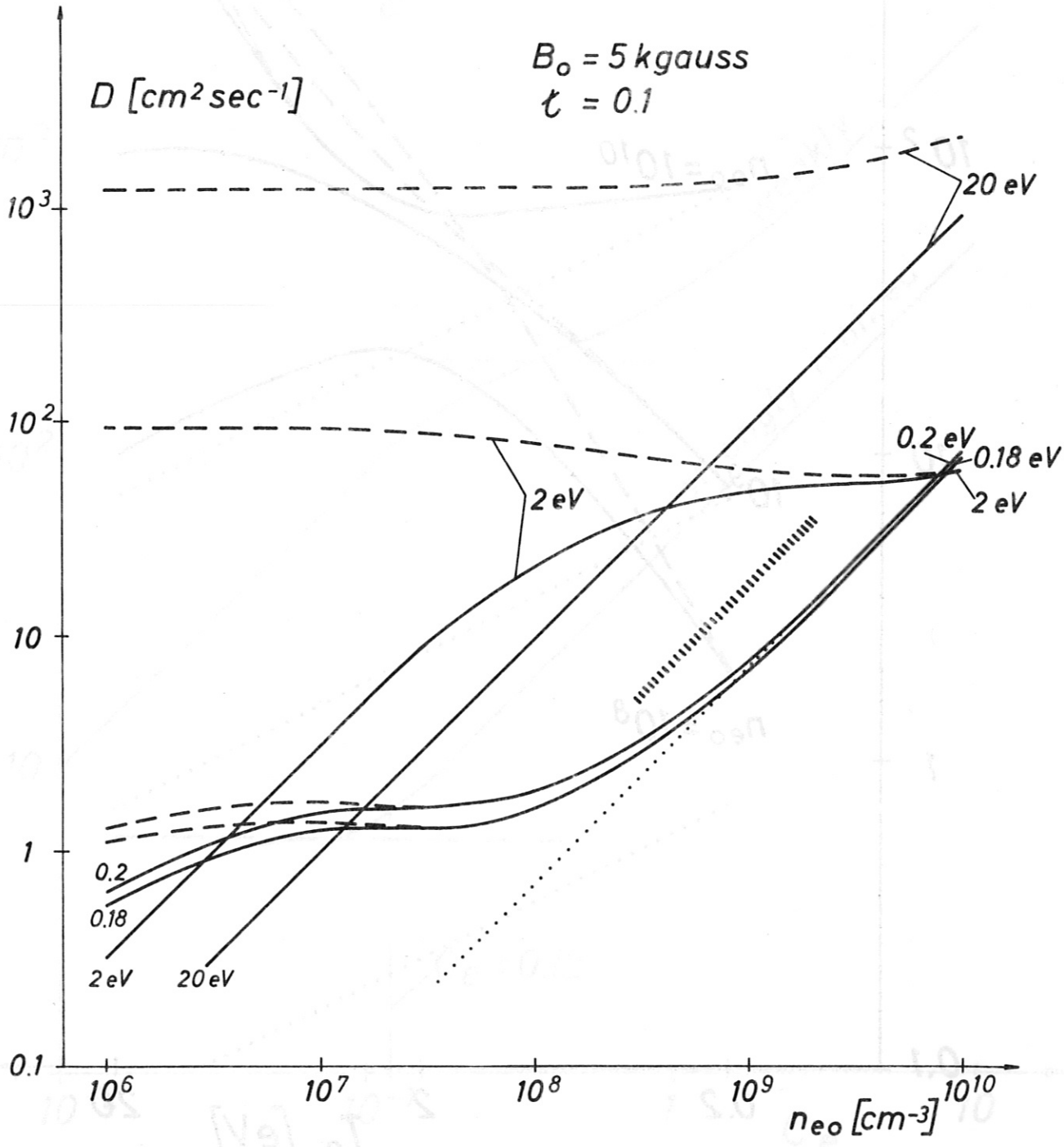
D [cm² sec⁻¹]
B₀ = 5 kgauss
t = 0.1
10³
10²
10
1
0.1
20 eV
2 eV
0.2 eV
0.18 eV
2 eV
0.2
0.18
2 eV
20 eV
10⁶
10⁷
10⁸
10⁹
10¹⁰
n_eo [cm⁻³]

FIG. 1

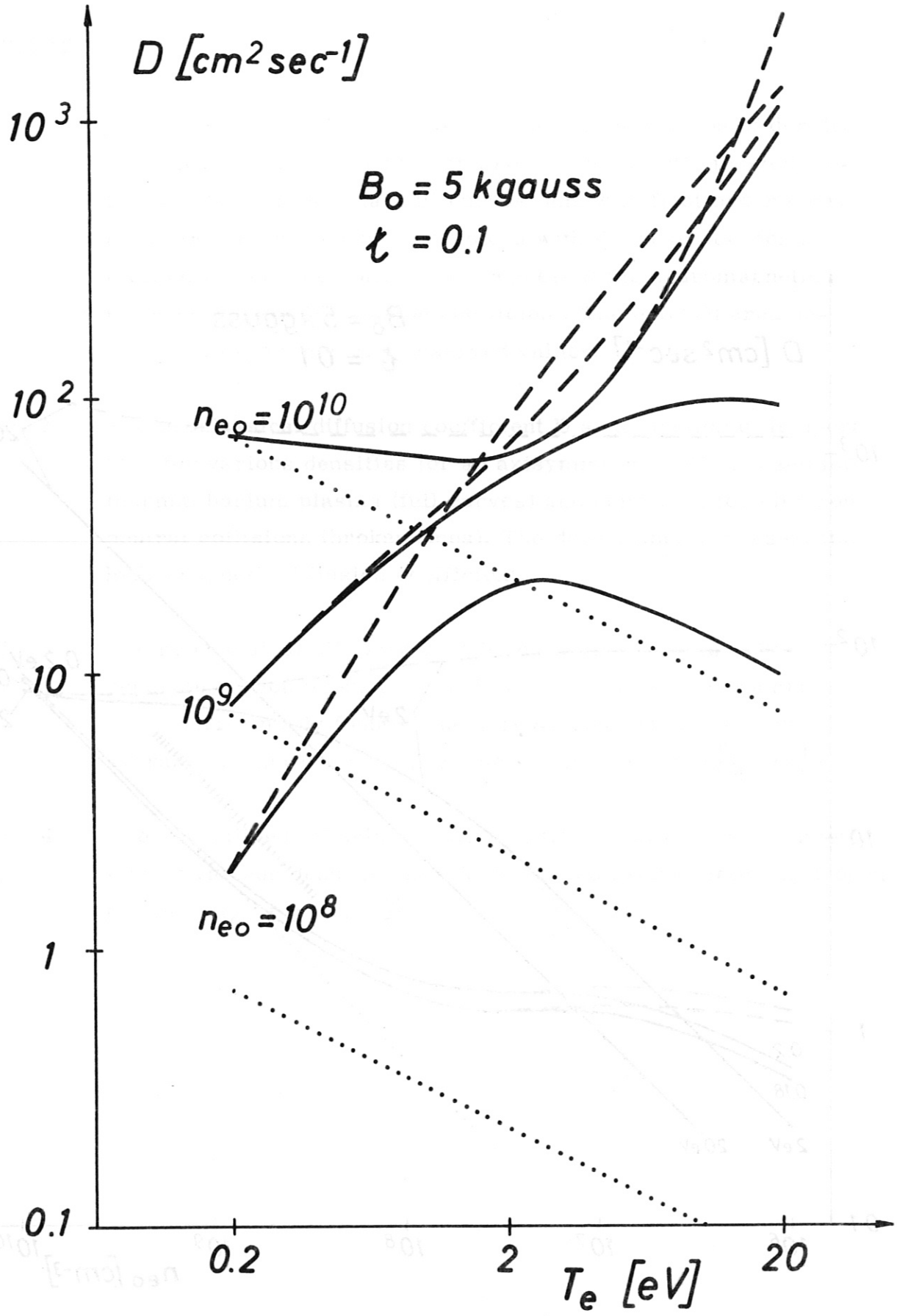
D [cm² sec⁻¹]
10³
10²
10
1
0.1
B₀ = 5 kgauss
t = 0.1
n_eo = 10¹⁰
10⁹
n_eo = 10⁸
0.2
2
20
T_e [eV]

FIG. 2

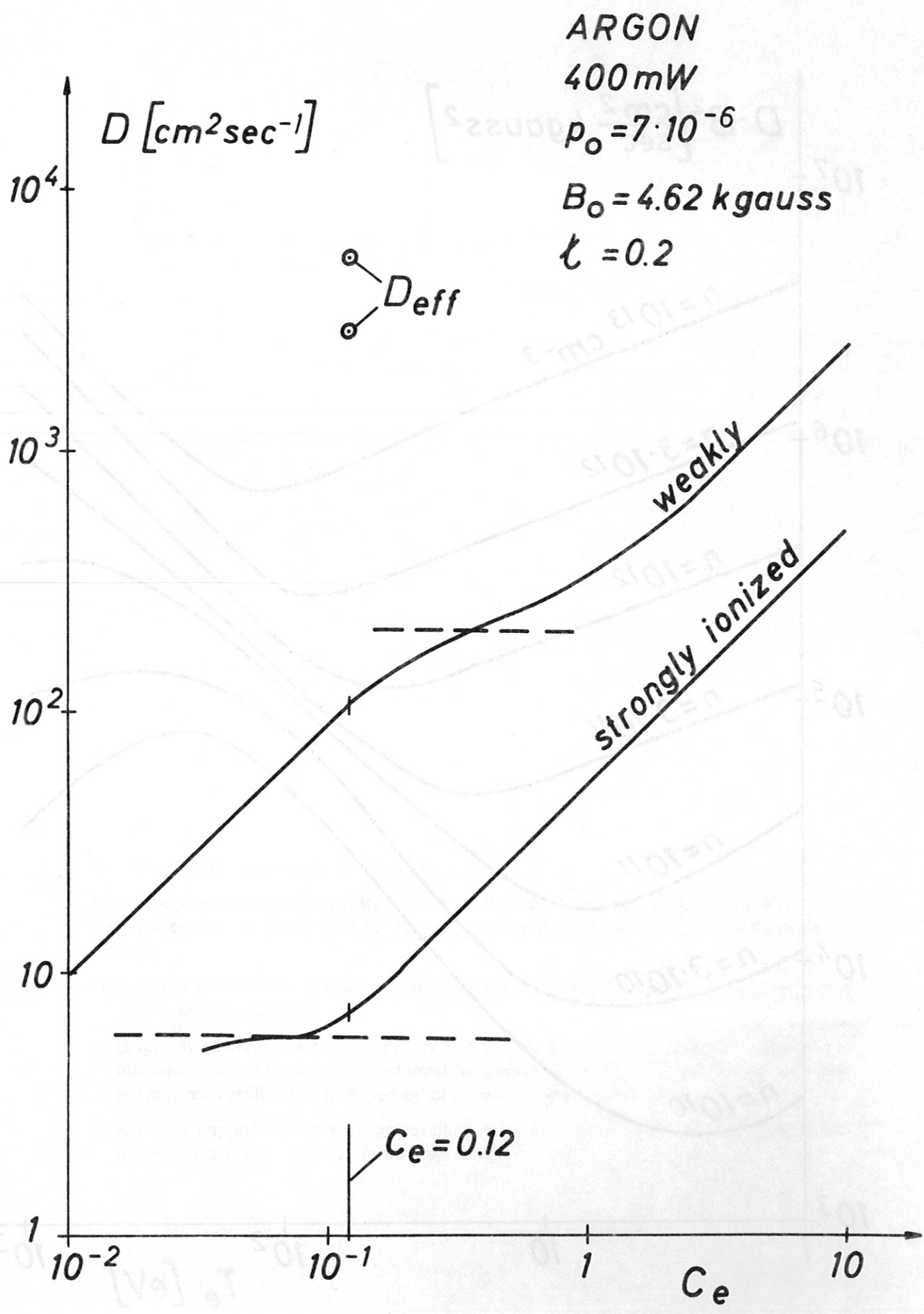
ARGON
400 mW
$p_o = 7 \cdot 10^{-6}$
$B_o = 4.62$ kgauss
$t = 0.2$
$D\ [cm^2 sec^{-1}]$
D_{eff}
10^4
10^3
10^2
10
1
weakly
strongly ionized
$C_e = 0.12$
10^{-2}
10^{-1}
1
10
C_e

FIG. 3

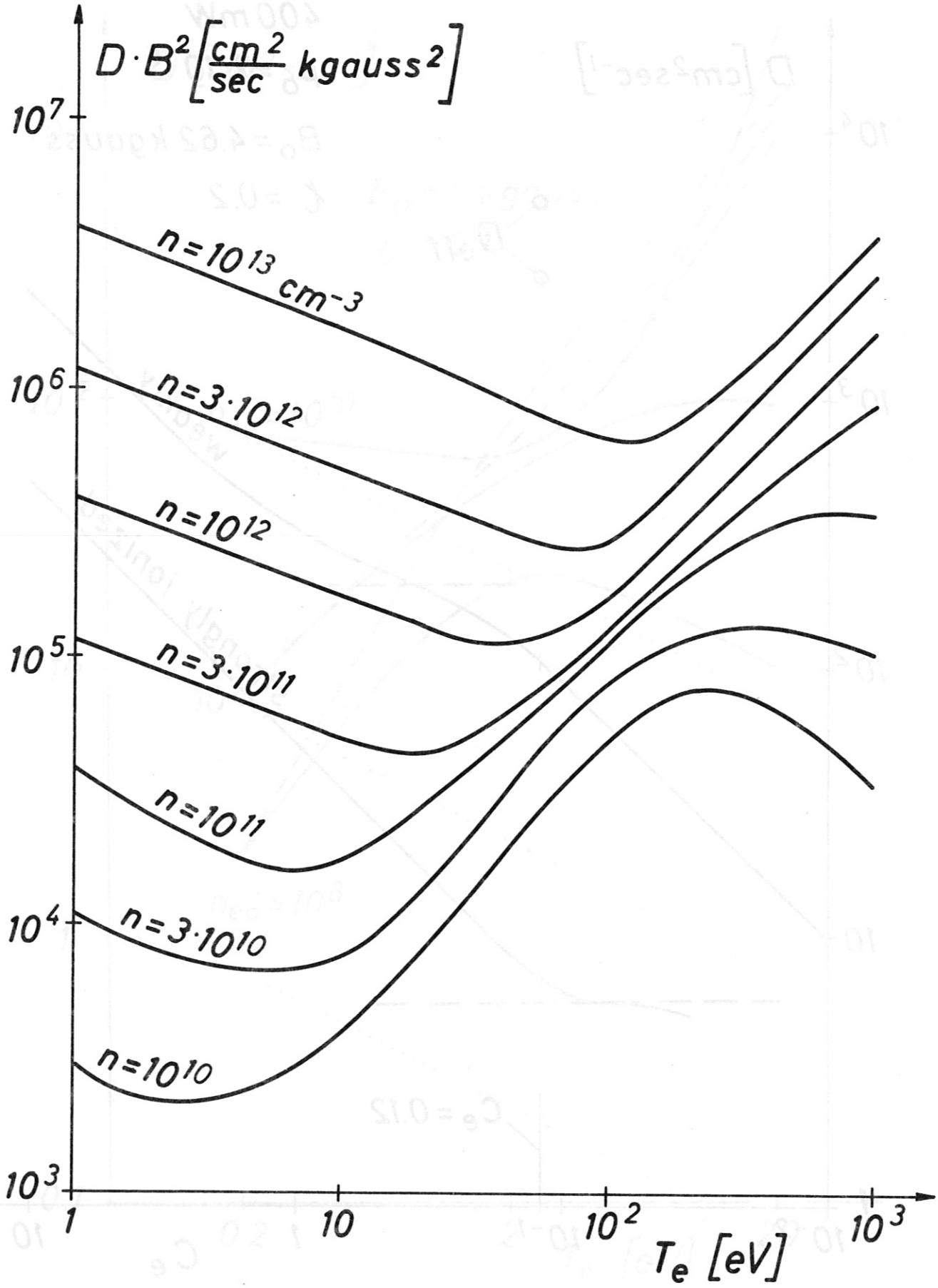
$D \cdot B^2 \left[\frac{cm^2}{sec}\ kgauss^2\right]$
10^7
10^6
10^5
10^4
10^3
$n=10^{13}\ cm^{-3}$
$n=3\cdot10^{12}$
$n=10^{12}$
$n=3\cdot10^{11}$
$n=10^{11}$
$n=3\cdot10^{10}$
$n=10^{10}$
1
10
10^2
10^3
T_e [eV]

FIG. 4